Table X. Cyclopropanes Heat of Vaporization Parameters[a]

| EQ | WT | $H_v$ (calcd) | $H_v$ (exptl) | difference (calcd - exptl)[b] | compound |
|---|---|---|---|---|---|
| 1 | 10 | 6.52 | 6.58 | -0.06 | spiropentane (7) |
| 2 | 10 | 6.04 | 6.00 | 0.04 | 1,1-dimethylcyclopropane (3) |
| 3 | 10 | 8.13 | 8.00 | 0.13 | bicyclopropyl (16) |
| 4 | 10 | 7.83 | 7.92 | -0.09 | bicyclo[3.1.0]hexane (10) |
| 5 | 10 | 9.11 | 8.84 | 0.27 | quadracyclane (20) |
| 6 | 10 | 8.74 | 9.17 | -0.43 | nortricyclane (14) |
| 7 | 10 | 8.95 | 9.12 | -0.17 | bicyclo[4.1.0]heptane (11) |
| 8 | 10 | 8.23 | 8.30 | -0.07 | 1-methylbicyclo[3.1.0]-hexane (26) |

Best Values

| | |
|---|---|
| S3 = 0.815 | (no. of secondary cyclopropane hydrogens) |
| T3 = 0.805 | (no. of tertiary cyclopropane hydrogens) |
| Pr3 = 0.463 | (no. of methylcyclopropane hydrogens) |
| C12 = 0.485 | (no. of cis-1,2-substitutions on a cyclopropane ring) |

[a] The formula and the parameters for cyclopentane and cyclohexane rings were taken from K. J. Laidler[78a] and E. G. Lovering et al.[78b] [b] Standard deviation 0.20.

and the C-H (5-22) bond increments have been given the same values as a $C(sp^3)$-$C(sp^3)$ (0.493) and $C(sp^3)$-H (-3.125), respectively (the MM3 values are 3.506 and -4.590). The other three parameters (corrections for different 22-22 types, and three-membered ring) were set to zero. With use of these parameters, together with the normal heat parameters and the calculated steric energies, reasonable strain energies (SI) could be calculated for the various polycyclic structures. Some examples are given in Table VI, and with use of a "strain per carbon atom" criteria, the following order (MM2) was found:

bicyclopropyl ≤ cyclopropane < bicyclo[2.1.0]pentane < spiropentane ≤ bicyclo[1.1.0]butane < quadracyclane < prismane

In the MM3 scheme, some extra strain has been attributed to the [1.1.0] structure (compounds **6** and **25**), in comparison with the various [2.1.0] ones (e.g., **8**, **18**, **20**). Hence bicyclobutane (**6**) precedes quadracyclane (**20**) in the above sequence.

## Conclusions

A new scheme and parameter set for cyclopropanes have been developed and incorporated into the MM2 and MM3 force fields. This improved treatment solves many of the deficiencies existing in earlier versions of MM2, and is superior to other, previously suggested, schemes.[2] Heats of formation for cyclopropanes are now calculated with the same degree of accuracy as for hydrocarbons in general. Due to a more detailed treatment of the angles ($\theta_0$) in the fused and spiro small ring structures in MM3, the latter performs a little better in reproducing the experimental (especially MW-based) geometries.[82]

**Acknowledgment.** We are indebted to the National Institutes of Health (Grant No. R24 RR02165), the National Science Foundation (Grant No. CHE 8614548), and Glaxo Inc. for support of this work.

**Registry No. 1**, 75-19-4; **2**, 594-11-6; **3**, 1630-94-0; **4a**, 2402-06-4; **4b**, 930-18-7; **5**, 1191-96-4; **6**, 157-33-5; **7**, 157-40-4; **8**, 185-94-4; **9a**, 50338-80-2; **9b**, 30163-38-3; **10**, 285-58-5; **11**, 286-08-8; **14**, 279-19-6; **15**, 26902-55-6; **16**, 5685-46-1; **17a**, 50895-58-4; **17b**, 50695-42-6; **18b**, 21531-33-9; **19a**, 650-42-0; **20**, 278-06-8; **21**, 24375-17-5; **22a**, 103495-76-7; **23**, 59020-33-6; **24**, 174-73-2; **25**, 930-25-6; **26**, 4625-24-5; **27**, 286-43-1; **28**, 286-60-2.

(82) After the completion of this study, we were notified of preliminary results of MO ab initio calculations that have been done on bitetrahedryl (**34** in Figure 1).[79] This is a very interesting example for the short, exocyclic, 22-22 bond, since from theoretical considerations, the bond connecting the two tetrahedrane moieties is expected to be the shortest one possible for saturated hydrocarbons. The ab initio calculated bond length was 1.449 (STO-3G) or 1.444 Å (DZ+P). MM3 gives a bond length of 1.449 Å, in good agreement with the MO results. It should be stated that MM2 fails to give the correct geometry of bitetrahedryl, as well as its parent compound tetrahedrane: The large difference between the natural and the actual CCH bond angle causes the whole MM2 structure to converge into a nonsymmetric form. This is avoided in MM3 due to the angle corrections mechanism, which reduces the above gap, while still keeping it large enough to reproduce the extreme shortening of the central (as well as other) bonds. Tetrahedrane and bitetrahedryl were not used in the MM3 parametrization as these ab initio results were obtained after the parametrization was completed.

# Theoretical Study of the Reactions of Pentacoordinated Trigonal-Bipyramidal Compounds: $PH_5$, $PF_5$, $PF_4H$, $PF_3H_2$, $PF_4CH_3$, $PF_3(CH_3)_2$, $P(O_2C_2H_4)H_3$, $P(OC_3H_6)H_3$, and $PO_5H_4^-$

**H. Wasada*,† and K. Hirao‡**

*Contribution from the Department of Chemistry, Faculty of Science, Nagoya University, Nagoya, Japan, Department of Chemistry, College of General Education, Nagoya University, Nagoya, Japan, and Institute for Molecular Science, Okazaki, Japan.* *Received November 28, 1990*

**Abstract:** We have studied pseudorotation reactions of some pentacoordinated phosphorus compounds [$PH_5$, $PF_5$, $PF_4H$, $PF_3H_2$, $PF_4CH_3$, $PF_3(CH_3)_2$, $P(O_2C_2H_4)H_3$, $P(OC_3H_6)H_3$, and $PO_5H_4^-$] to elucidate the reaction mechanisms by using ab initio SCF and MP4 methods. We have calculated the potential surface for the lowest pass of pseudorotation reactions. The geometries of the transition state connecting them have been determined theoretically. The ligands which form the covalent bond with the central phosphorus atom such as hydrogen, methyl, and methylene groups prefer to coordinate in the equatorial position. This nature of the ligands is called as the *equatoriphilicity*. It is possible to predict whether the pseudorotation reaction can occur or not, based on the number of the equatoriphilic ligands in the pentacoordinated molecules. The normal coordinate analyses have been carried out at the stationary points of $PH_5$ and $PF_5$. The mechanism of pseudorotation is discussed and explained on a theoretical basis.

## 1. Introduction

The different behavior in the hydrolysis reaction between DNA and RNA is an interesting fact related to their different roles in the biochemical system. DNA molecules, which work as tapes for the storage of genetic information show very strong resistance to the decomposition by hydrolysis. Even after a 1-h reaction at 100 °C in 1 N NaOH (aq) DNA molecules do not show any changes.[1] On the other hand, 2-hydroxyethyl methyl phosphate,

† Faculty of Science, Nagoya University.
‡ College of General Education, Nagoya University and Institute for Molecular Science.

(1) Dugas, H.; Penney, C. *Bioorganic Chemistry. A Chemical Approach to Enzyme Action*; Springer-Verlag: New York, 1981.

0002-7863/92/1514-16$03.00/0 

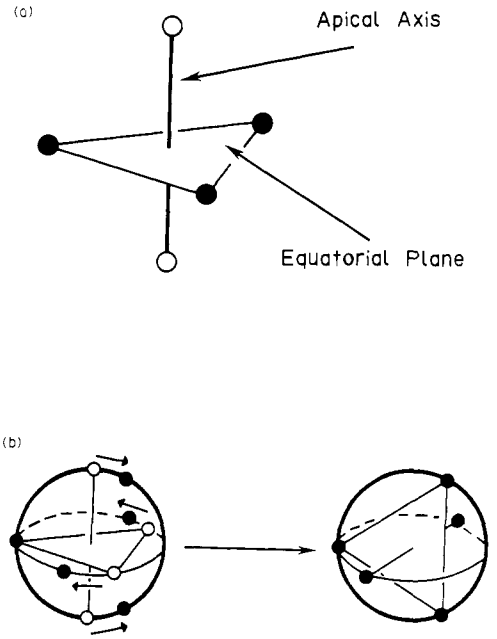


**Figure 1.** (a) Schematic structure of $D_{3h}$ trigonal bipyramid. (b) Schematic explanation for Berry's pseudorotation reaction.

which is a model molecule of RNA, easily undergoes the hydrolysis reaction. The half-life of the hydrolysis reaction of this molecule at 25 °C in 1 N NaOH (aq) is 25 min.[1] Indeed RNA molecules have high turnover rates and are easily hydrolyzed. The difference in the hydrolysis reaction between DNA and RNA which functions as a carrier of genetic information comes from these chemical characteristics. The behavior of phosphate ester to the hydrolysis reaction is closely related to the nature of the phosphorus atom. The high reactivity comes from the pentacoordinated intermediate formed by the attack of the vicinal hydroxyl group through the hydrolysis reaction. The group-15 elements in the second and succeeding rows of the periodic table can show higher valence numbers. One of the possible structures of pentacoordinated compounds is trigonal bipyramid. The hypervalent character of elements in higher rows of the periodic table is quite different from that of the first-row elements. For example, $CH_5^-$ is in a high-energy transition state of the $S_N2$ reaction, while $SiH_5^-$ is a stable intermediate. Recently, as theoretical techniques have been expanded, it becomes possible to predict the existence of compounds from a theoretical background. Though it has been assumed that hypervalent compounds of first-row elements such as nitrogen cannot exist, a recent study of Ewig et al. suggested the existence of three pentacoordinated nitrogen compounds, i.e., $NF_3H_2$, $NF_4H$, and $NF_5$.[53]

In relation to the pentacoordinated phosphorus compounds, Westheimer[2] has proposed the mechanism of the hydrolysis of phosphate esters. He postulated that the nucleophilic displacement reactions of phosphorus compounds proceed through pentacoordinated intermediates (see Figure 1a). He also assumed that an axial entry of the nucleophile takes place in forming a trigonal-bipyramidal intermediate and that an axial departure of a leaving group occurs in forming products. If the activated states have sufficiently long lifetimes, it is further assumed that ligand rearrangement, that is, pseudorotation reaction, may be encountered before product formation. Berry's pseudorotation[4] process, which rapidly exchanges axial and equatorial ligands in the trigonal-bipyramidal intermediate (Figure 1b), has a strong basis in phosphorus chemistry where NMR studies have established an intramolecular ligand-exchange process for many phosphorus molecules (see Figure 2). Many studies of the bonding nature, structures of phosphorus molecules, and relative reaction energies of the pseudorotation have been performed experimentally and theoretically.[3-32,46-50,55-58] Particularly, Holmes has contributed to developments of the understanding of pentacoordinated phosphorus compounds.[32] In theoretical treatments some models are adopted: a valence electron pair repulsion model[24] and a three-center four-electron bonding model.[25-27] Furthermore, there are many ab initio or semiempirical molecular orbital calculations.[27-31,50] Strich et al.[7] studied $PH_5$ and supported Berry's pseudorotation. Marsden[12] calculated $PF_5$ and estimated the energy barrier of the pseudorotation to be 3.8 kcal/mol. Schleyer[45] studied first- and second-row substituents of phosphoranes in a systematic way. Recently, Dieters and Holmes[14] studied a series of substituted phosphorus compounds. The pseudorotation reaction is not confined to only phosphorus compounds. Recently, Gordon et al.[50,59] performed theoretically a series of study on the pseudorotation reactions of $SiH_5^-$ and $SiH_4F^-$.

There has been much interest in the pseudorotation mechanism in view of the important role of the phosphorus chemistry. As the pseudorotation reaction is a ligand-exchange isomerization between the apical part and the equatorial part, the reaction mechanism is closely related to the relative stabilities between the isomers which are interconverted through the pseudorotation. The relative stabilities of apical and equatorial substituted isomers have been discussed by substituent electronegativities, steric interaction, and ring strain. It is very difficult to observe directly the pseudorotation process as it is a reaction in the intermediate. And it is necessary to study the transition state of the reaction to understand the process of the pseudorotation reaction. Ab initio calculations are nowadays widely accepted as a legitimate way of getting information that is experimentally inaccessible. The theory can describe the mechanism and provide some correct explanations of the pseudorotation hypothesis.

(2) Westheimer, F. H. *Acc. Chem. Res.* **1968**, *1*, 70.
(3) Ugi, I.; Ramirez, F.; Marquarding, D.; Klusacek, H.; Gokel, G.; Gillespie, P. *Angew. Chem.* **1970**, *82*, 766.
(4) Berry, R. S. *J. Chem. Phys.* **1960**, *32*, 933.
(5) Hoffmann, R.; Howell, J. M.; Muetterties, E. L. *J. Am. Chem. Soc.* **1972**, *94*, 3047.
(6) Florey, J. B.; Cusachs, L. C. *J. Am. Chem. Soc.* **1972**, *94*, 3040.
(7) Strich, A.; Veillard, A. *J. Am. Chem. Soc.* **1973**, *95*, 5574.
(8) Keil, F.; Kutzelnigg, W. *J. Am. Chem. Soc.* **1975**, *97*, 3623.
(9) Holmes, R. R. *J. Am. Chem. Soc.* **1978**, *100*, 433.
(10) Kutzelnigg, W.; Wallmeier, H. *Theor. Chim. Acta* **1979**, *51*, 261.
(11) Trinquier, G.; Daudey, J.-P.; Caruana, G.; Madaule, Y. *J. Am. Chem. Soc.* **1984**, *106*, 4794.
(12) Marsden, C. J. *J. Chem. Soc., Chem. Commun.* **1984**, 401.
(13) de Keijzer, A. E. H.; Koole, L. H.; Buck, H. M. *J. Am. Chem. Soc.* **1988**, *110*, 5995.
(14) Deiters, J. A.; Holmes, R. R.; Holmes, J. M. *J. Am. Chem. Soc.* **1988**, *110*, 7672.
(15) Anslyn, E.; Breslow, R. *J. Am. Chem. Soc.* **1989**, *111*, 4473.
(16) Bartell, L. S.; Hansen, K. W. *Inorg. Chem.* **1965**, *4*, 1777.
(17) Muetterties, E. L.; Mahler, W.; Schmutzler, R. *Inorg. Chem.* **1963**, *2*, 613.
(18) Muetterties, E. L.; Mahler, W.; Packer, K. J.; Schmutzler, R. *Inorg. Chem.* **1964**, *3*, 1298.
(19) Schmutzler, R.; Reddy, G. S. *Inorg. Chem.* **1965**, *4*, 191.
(20) Schmutzler, R. *J. Am. Chem. Soc.* **1964**, *86*, 4500.
(21) Rauk, A.; Allen, L. C.; Mislow, K. *J. Am. Chem. Soc.* **1972**, *94*, 3035.
(22) Kutzelnigg, W.; Wasilewski, J. *J. Am. Chem. Soc.* **1982**, *104*, 953.
(23) McDowell, R. S.; Streitwieser, A., Jr. *J. Am. Chem. Soc.* **1985**, *107*, 5849.
(24) Gillespie, R. J. *Molecular Geometry*; Van Nostrand-Reinhold: London, 1972.
(25) Rundle, R. E. *J. Am. Chem. Soc.* **1963**, *85*, 112.
(26) Rundle, R. E. *Prog. Chem.* **1963**, *1*, 81.
(27) Hach, R. J.; Rundle, R. E. *J. Am. Chem. Soc.* **1951**, *73*, 4321.
(28) Hoffmann, R.; Howell, J. M.; Rossi, A. R. *J. Am. Chem. Soc.* **1976**, *98*, 2484.
(29) Howell, J. M. *J. Am. Chem. Soc.* **1977**, *99*, 7447.
(30) Krogh-Jespersen, M.-B.; Chandrasekhar, J.; Wurthwein, E. U.; Collins, J. B.; Schleyer, P. v. R. *J. Am. Chem. Soc.* **1980**, *102*, 2263.
(31) Holmes, R. R. *J. Am. Chem. Soc.* **1984**, *106*, 3745.
(32) Holmes, R. R. *Pentacoordinated Phosphorus*; ACS Monograph Series 175 and 176; American Chemical Society: Washington, DC, 1980; Vols. 1 and 2.

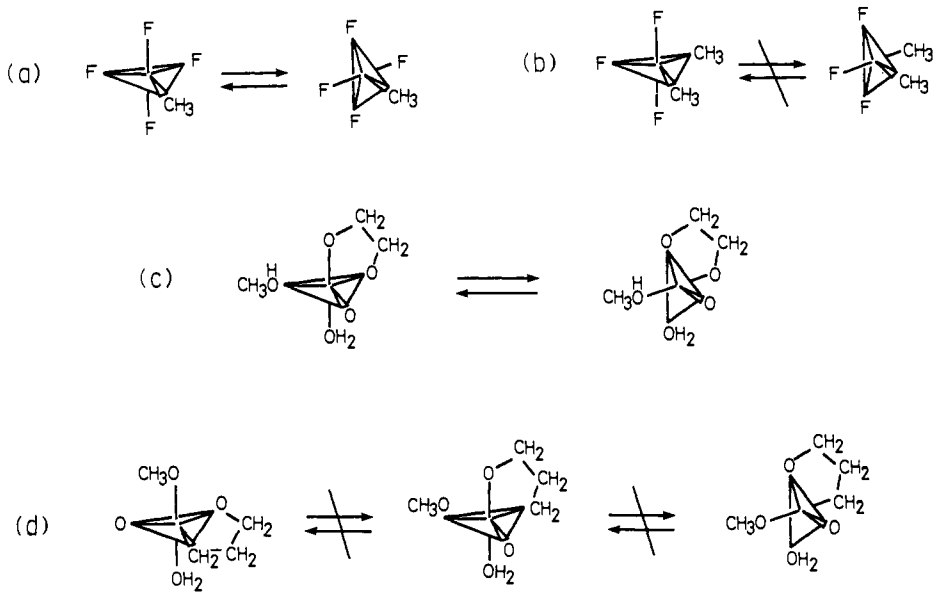

Figure 2. Experimental results of some pseudorotation reactions.

We have carried out ab initio molecular orbital calculations on pseudorotation profiles of some phosphorus compounds in this study. The computational methods in this study are described in section 2. The results are discussed in section 3. The emphasis of the discussion is put on the pseudorotation mechanism. We also discuss the relative stability of isomers. The equatorial substituent effects in the apical bond formation are also discussed. Some general conclusions are summarized in section 4.

## 2. Computational Details

In this study all geometries of pentacoordinated compounds were fully optimized at the SCF level. Because of the fact pointed out by Magnusson[44] that relative energies of singly substituted phosphoranes vary considerably with different basis set, it is necessary to use a basis set at least as large as 6-31G*. So for all molecules except $PH_5$, the basis sets used are in the double-zeta level[33,35] which are augmented with polarization functions. The polarization functions ($\alpha_P = 0.43$, $\alpha_C = 0.75$, $\alpha_O = 0.85$, $\alpha_F = 0.90$, $\alpha_H = 1.00$) were added to the phosphorus atom and other ligands which are directly connected to the central phosphorus atom. We have also added a diffuse function ($\alpha_O = 0.059$) on the phosphoryl oxygen atom in the calculation of $PO_5H_4^-$. We used a triple-zeta[33,54] plus polarization (TZP) basis set for $PH_5$ calculations. The correlation energies were calculated by the fourth-order Møller–Plesset perturbation method (MP4) at SCF optimized geometries.

## 3. Results and Discussion

In section 3.A we discuss the pseudorotation of some pentacoordinated phosphorus compounds. We consider the relation between the stability and the structure of pentacoordinated phosphorus compound in section 3.B, i.e., equatoriphilicity. We discuss the apical bond character by using the orbital energy correlation diagrams in section 3.C. Some discussions on the equatorial substituent effects are given in section 3.D.

**A. Pseudorotation. $PH_5$.** The optimized structures of the ground ($D_{3h}$) and transition ($C_{4v}$) states are shown in Figure 3, a and b, respectively. The ligand at the apex position of the $C_{4v}$ structure is called as the pivotal ligand.

The energy relation between the ground state and the transition state is shown in the energy diagram (see Figure 4). The broken line shows the result of the SCF calculation, and the solid shows that of the MP4 calculation. The individual electron pairs are separated as far as possible in the ground state. These electrons become closer to each other in the transition state. Thus the

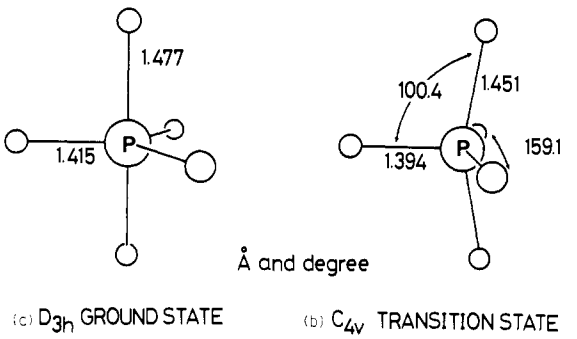


Figure 3. Optimized structure of $PH_5$: (a) ground-state structure, (b) transition-state structure of the pseudorotation reaction. The bond length is shown in Å and the angle in degrees.

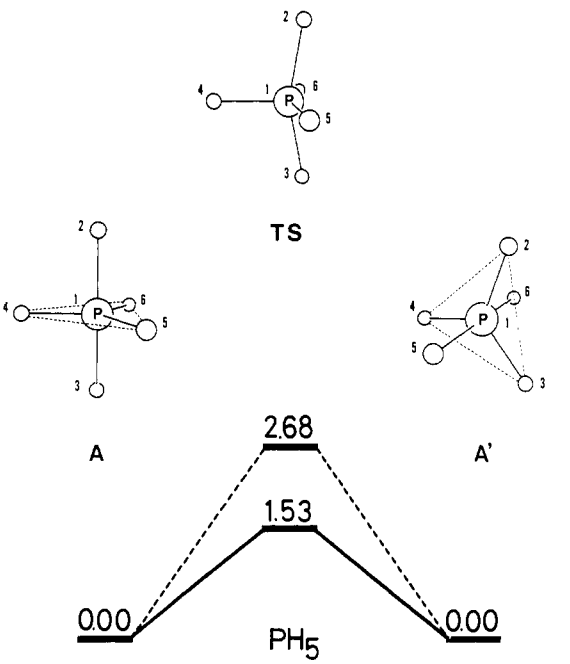


Figure 4. Energy diagram for the pseudorotation reaction of $PH_5$. TS means the transition state with $C_{4v}$ symmetry. The energies are relative to that of A in kcal/mol: (---) SCF, (—) MP4. The SCF energy of the ground state A is −343.528 616 hartrees.

(33) Dunning, T. H., Jr. *J. Chem. Phys.* **1970**, *53*, 2823.
(34) Frisch, M. J.; Binkley, J. S.; Schlegel, H. B.; Raghavachari, K.; Melius, C. F.; Martin, R. L.; Stewart, J. J. P.; Bobrowicz, F. W.; Rohlfing, C. M.; Kahn, L. R.; Defrees, D. J.; Seeger, R.; Whiteside, R. A.; Fox, F. J.; Fluder, E. M.; Topiol, S.; Pople, J. A. *Gaussian 86*; Carnegie-Mellon Quantum Chemistry Publishing Unit, Carnegie-Mellon University: Pittsburg, PA.
(35) Dunning, T. H., Jr.; Hay, P. J. *Modern Theoretical Chemistry*, Schaefer, H. F., III, Ed.; Plenum Press: New York, 1977; Vol. 3, p 1.

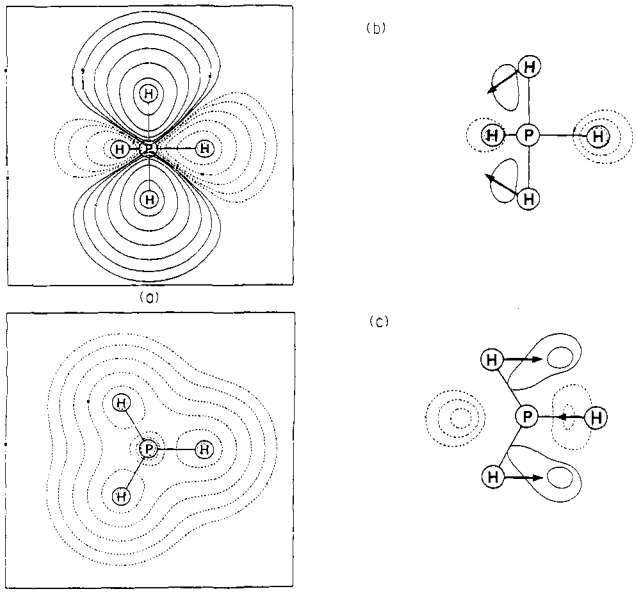


**Figure 5.** (a) Contour map of the highest occupied molecular orbital of $PH_5$. (b) Calculated transition density from HOMO to LUMO of $PH_5$ molecule along the apical axis. (c) Transition density in the equatorial plane. The expected intramolecular movements of atoms are shown by arrows.

electron correlation effect becomes more significant in the transition state. The energy barrier of the pseudorotation reaction is about 2 kcal/mol with and without the electron correlation. We can say, therefore, that Berry's pseudorotation occurs very easily in this molecule.

The electronic structure of phosphorane $PH_5$ is

$$(\text{core})^{10}(1a_1')^2(1e')^2(2e')^2(1a_2'')^2(2a_1')^2(3e')^0(4e')^0(3a_1')^0$$

The highest occupied molecular orbital (HOMO) is shown in Figure 5a. The apical bond has a three-center character and is weaker than the normal single bond. The electronic structure of the transition state is

$$(\text{core})^{10}(1a_1)^2(1e)^2(2e)^2(2a_1)^2(1b_1)^2(3a_1)^0(4a_1)^0$$

The changes of the bond length of $PH_5$ through the reaction are shown in Table IIIa, in which the bond length before the reaction is put as 100. The pivotal ligand stays in the equatorial plane before and after the pseudorotation reaction. The pivotal bond length is shortest in the transition state. Its change is also smallest in the reaction. The orbital mainly related to the pivot is $1a_1$ MO which is the deepest one in the valence molecular orbitals of the ground state. In the transition state two apical orbitals and two equatorial orbitals mix up to form four equivalent ligand orbitals. The bond brought to the apical position is lengthened. The electron density moves to the overlap region between phosphorus and the pivotal hydrogen from other parts of the molecule in the course of the reaction, so the pivotal bond becomes shorter than the corresponding equatorial bonds in the ground state.

The symmetry of the transition density[36-41] from the HOMO to the LUMO of the ground state $PH_5$ is

$$a_1' \times e' = e'$$

The intramolecular vibration mode inducing the pseudorotation is e′ symmetry. The transition densities with 3-21G* basis set are shown in Figure 5, b and c, in which (b) is one along the apical axis and (c) is one in the equatorial plane. The intramolecular displacement of individual atoms is expected to occur along the arrows. The results of the vibrational analysis of the ground state with the TZP basis set are shown in Figure 6, a and b. There are two modes of e′ symmetry with frequencies of 629.0 $cm^{-1}$ and 1373.8 $cm^{-1}$. We can see that the bending of the equatorial bond angle is easier than that of the apical one, and the opening motion of the equatorial ligands (629.0 $cm^{-1}$) initiates the pseudorotation reaction. We also performed the vibrational analysis calculation for the transition state. There is one vibrational mode with the imaginary frequency. The transition vector is shown in Figure 6c. One of the HPH angles closes down and the other angle opens up simultaneously. The transition vector shows that the molecule returns to the ground state along this mode of the vibration.

**$PF_5$.** The optimized structures of $PF_5$ are shown in Figure 7. This molecule has a $D_{3h}$ symmetry in the ground state and a $C_{4v}$ in the transition state. The values in parentheses are the experimental ones.[16] The calculated apical and equatorial bond lengths are in good agreement with experiment. The calculated energies at several levels of approximation for ground and transition states are shown in Table I. From these results, the MP2 level of correlation correction seems to be adequate for the calculation of the potential energy barrier. The potential energy barrier in the reaction has 4.24–5.07 kcal/mol (see Figure 8), so the pseudorotation reaction proceeds easily. The change of the bond length is least for the pivotal ligand as shown in Table IIIb. The bond length of the pivotal ligand is shortest in the transition-state-like $PH_5$ case.

The results of the vibrational analysis are shown in Figure 9. Berry's pseudorotation reaction begins with e′ vibration and the transition state has $C_{4v}$ symmetry. The opening motion of the equatorial ligand is easier (185.3 $cm^{-1}$) than the bending of the apical bond (559.9 $cm^{-1}$) for this molecule as well as $PH_5$.

**$PF_4H$ and $PF_3H_2$.** The total and relative energies are summarized in Table I for $PF_4H$ and $PF_3H_2$. The energy diagram of $PF_4H$ in the course of the reaction is drawn in Figure 10a. The hydrogen atom is in the equatorial position in the ground state. This atom occupies the apex (pivotal position) of the $C_{4v}$ structure in the transition state. There are 7.38 and 5.70 kcal/mol of potential energy barriers for the pseudorotation reaction of $PF_4H$ at SCF and MP4 levels, respectively.

The most stable isomer of $PF_3H_2$ has two hydrogens in the equatorial position. The results of the calculated potential energy are summarized in Table II. The potential energy surface of this reaction is shown in Figure 10b. The isomerization product is fairly unstable because of the very small energy difference between

(36) Bader, R. F. W. *Can. J. Chem.* **1962**, *40*, 1164.
(37) Pearson, R. G. *J. Am. Chem. Soc.* **1969**, *91*, 1252.
(38) Pearson, R. G. *J. Am. Chem. Soc.* **1969**, *91*, 4947.
(39) Pearson, R. G. *J. Chem. Phys.* **1970**, *52*, 2167.
(40) Ballhausen, C. J. *J. Chem. Phys.* **1970**, *53*, 2986.
(41) Pearson, R. G. *J. Am. Chem. Soc.* **1972**, *94*, 8287.
(42) Pople, J. A., et al. *QCPE* No. 406; No. 437.
(43) Binkley, J. S.; Frisch, M. J.; Defrees, D. J.; Raghavachari, K.; Whiteside, R. A.; Schlegel, H. B.; Pople, J. A.; GAUSSIAN 82; Carnegie-Mellon Quantum Chemistry Publishing Unit, Carnegie-Mellon University: Pittsburgh, PA, 1984.
(44) Magnusson, E. *J. Comput. Chem.* **1984**, *5*, 612.
(45) Schleyer, P. v. R. *Pure Appl. Chem.* **1987**, *59*, 1647.
(46) Lemmen, P.; Baumgartner, R.; Ugi, I.; Ramirez, F. *Chem. Scr.* **1988**, *28*, 451.
(47) Auf der Heyde, T. P. E.; Bürgi, H.-B. *Inorg. Chem.* **1989**, *28*, 3982.
(48) Kutzelnigg, W.; Wasilewski, J. *J. Am. Chem. Soc.* **1982**, *104*, 953.
(49) Altmann, J. A.; Yates, K.; Csizmadia, I. G. *J. Am. Chem. Soc.* **1976**, *98*, 1450.
(50) Gordon, M. S.; Windus, T. L.; Burggraf, L. W.; Davis, L. P. *J. Am. Chem. Soc.* **1990**, *112*, 7167.
(51) Minkin, V. I.; Simkin, B. Ya.; Minyaev, R. M. *Quantum Chemistry of Organic Compounds*; Springer-Verlag: New York, 1990.
(52) Atkins, P. W. *Physical Chemistry*; Oxford University Press: Oxford, 1987.
(53) Ewig, C. S.; Van Wazer, J. R. *J. Am. Chem. Soc.* **1989**, *111*, 4172.
(54) Poirier, R.; Kari, R.; Csizmadia, I. G. *Handbook of Gaussian Basis Sets. A Compendium of ab Initio Molecular Orbital Calculations*; Elsevier; New York, 1985.
(55) Lim, C.; Karplus, M. *J. Am. Chem. Soc.* **1990**, *112*, 5872.
(56) Kluger, R.; Taylor, S. D. *J. Am. Chem. Soc.* **1990**, *112*, 6669.
(57) Uchimaru, T.; Tanabe, K.; Nishikawa, S.; Taira, K. *J. Am. Chem. Soc.* **1991**, *113*, 4351.
(58) Dejaegere, A.; Lim, C.; Karplus, M. *J. Am. Chem. Soc.* **1991**, *113*, 4353.
(59) Windus, T. L.; Gordon, M. S.; Burggraf, L. W.; Davis, L. P. *J. Am. Chem. Soc.* **1991**, *113*, 4356.

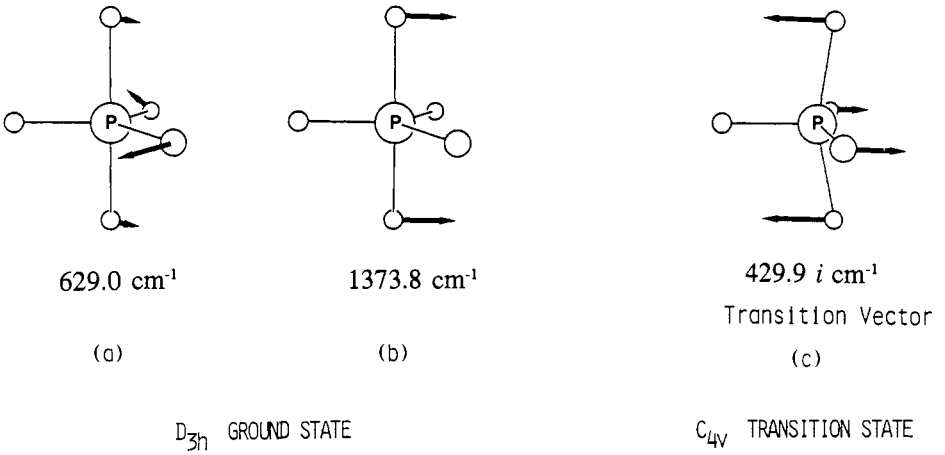


**Figure 6.** Vibrational modes of the $PH_5$ molecule: (a) and (b) e′ modes of the ground state and (c) the transition vector.

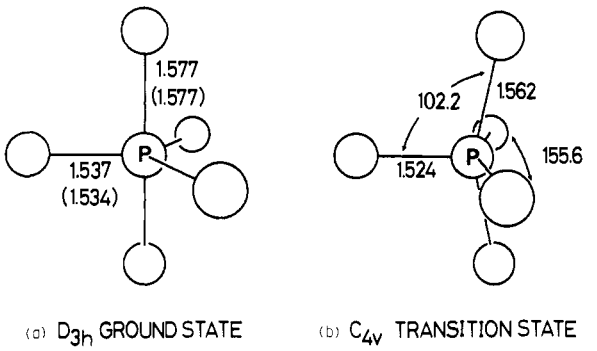


**Figure 7.** Optimized structures of the $PF_5$ molecule: (a) ground-state structure, and (b) transition-state structure. The values in the parentheses are experimental values.[16] The bond length is shown in Å and the angle in degrees.

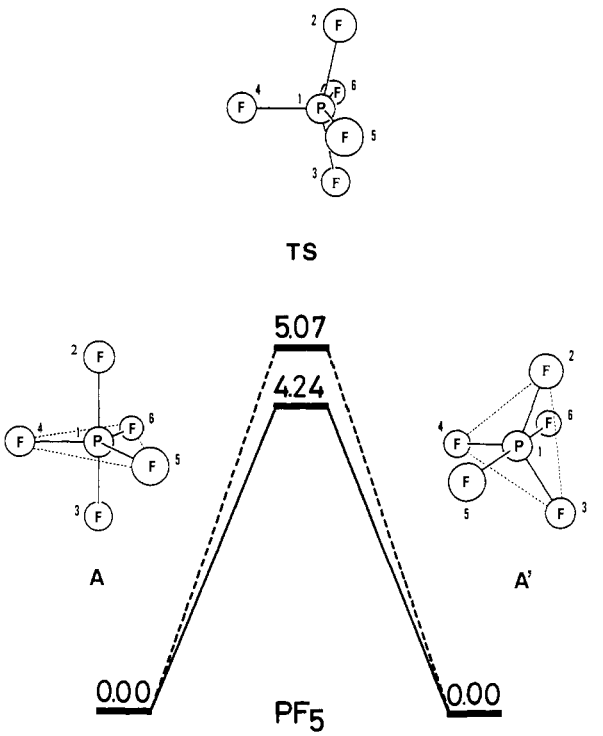


**Figure 8.** Energy diagram for the pseudorotation reaction of $PF_5$. The energies are relative to that of A in kcal/mol: (---) SCF, (—) MP4. The SCF energy of the ground state A is −838.184055 hartrees.

the transition state and the product. The barrier height of the pseudorotation of $PF_3H_2$ is calculated to be 12.16 and 10.43 kcal/mol by the SCF and MP4, respectively. The relative energies of the pseudorotated isomer to the ground state are calculated

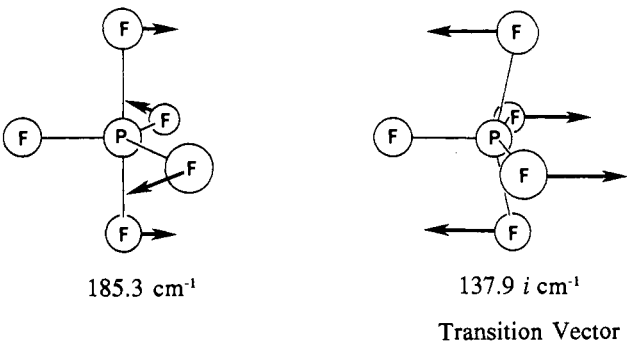


**Figure 9.** Vibrational modes of the $PF_5$ molecule: (a) e′ modes of the ground state and (b) the transition vector.

to be 12.03 and 10.82 kcal/mol at the SCF and MP4 levels, respectively. The isomerization reaction through the pseudorotation is fairly difficult to occur for $PF_3H_2$ because of the high potential energy barrier. We can also say that there is no stable energy minimum structure for the pseudorotation products from the MP4 results. Through the process of the pseudorotation reaction, both of two equatorial hydrogen atoms cannot remain in the equatorial plane. One hydrogen is brought inevitably to the apical position and its bond is lengthened, leading to instability of the molecular system.

**$PF_4CH_3$ and $PF_3(CH_3)_2$.** Westheimer discussed the pseudorotation reaction of $PF_4CH_3$ and $PF_3(CH_3)_2$.[2] If the pseudorotation reaction occurs, only one type of F-NMR peak is expected for $PF_4CH_3$. The NMR experiment verified that pseudorotation is expected to occur in the $PF_4CH_3$ molecule. On the other hand, no evidence of pseudorotation is obtained in $PF_3(CH_3)_2$.

Our results on $PF_4CH_3$ are shown in Figure 11a. One methyl group is in the equatorial plane at the ground state. The methyl group occupies the pivotal position in the transition-state structure. As the pseudorotation proceeds, two apical fluorines and two equatorial fluorines interchange. The energy barrier for the pseudorotation reaction is calculated to be 5.26 kcal/mol (SCF) and 3.95 kcal/mol (MP4). The easy proceeding of the pseudorotation reaction is expected for $PF_4CH_3$, which verifies experimental results.

We also studied $PF_3(CH_3)_2$. In the ground state two methyl groups occupy the equatorial positions. One of two methyl groups takes the apical position in the isomerization product. The other apical position is occupied by the fluorine atom. As the reaction proceeds, the bond brought to the apical position from the equatorial one is stretched, and the stability of the molecule decreases. The potential energy curve of the reaction is shown in Figure 11b. There is only one stable minimum structure for the $PF_3(CH_3)_2$ reaction. The energies of the isomerized product

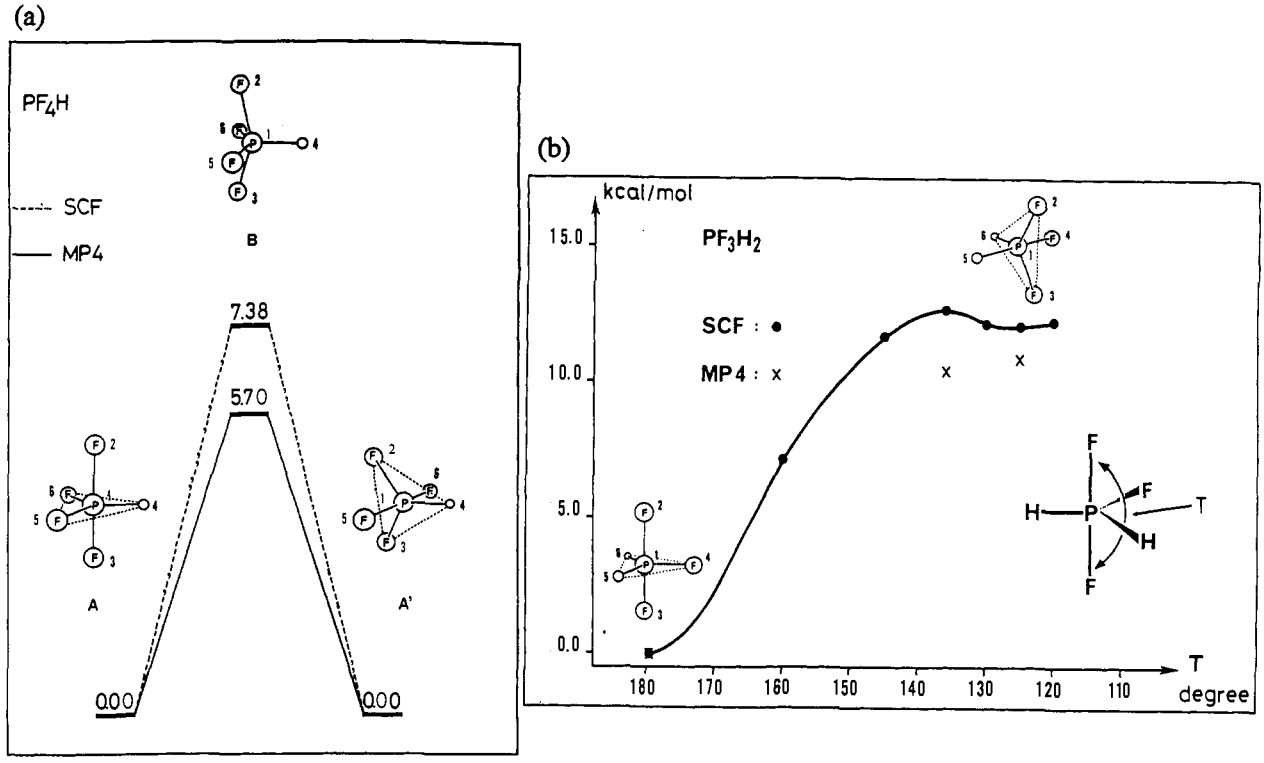


**Figure 10.** (a) The energy diagram for the pseudorotation reaction of $PF_4H$ in kcal/mol. The SCF energy of the ground state A is −739.263577 hartrees. (b) Potential energy curve of $PF_3H_2$ for the pseudorotation reaction in kcal/mol. One fluorine atom occupies an equatorial position in the ground state and two fluorine atoms occupy equatorial positions in the pseudorotated isomer. The SCF energy of the ground state is −640.339311 hartrees.

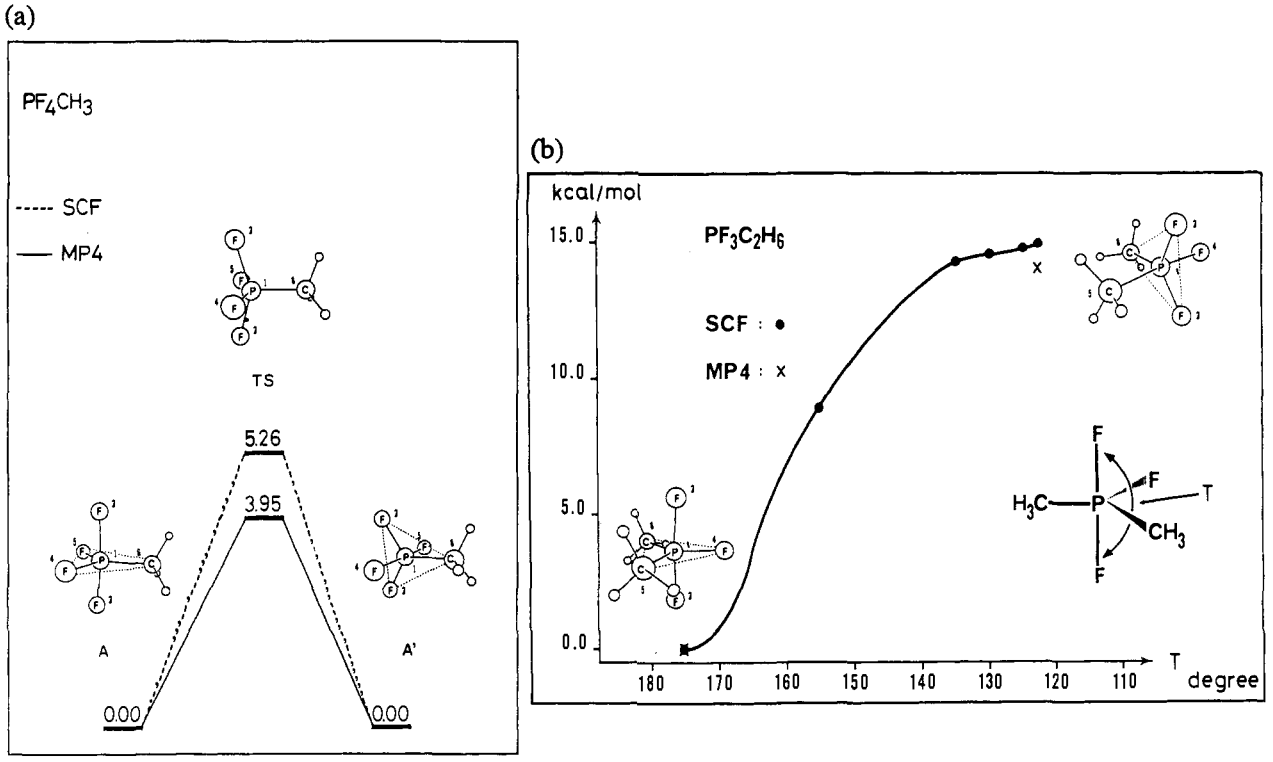


**Figure 11.** (a) Energy diagram for the pseudorotation reaction of $PF_4CH_3$ in kcal/mol. The SCF energy of the ground state A is −778.317482 hartrees. (b) The potential energy curve of $PF_3(CH_3)_2$ for the pseudorotation reaction in kcal/mol. The SCF energy of the ground state is −718.444972 hartrees.

are calculated to be 15.04 kcal/mol (SCF) and 14.01 kcal/mol (MP4) higher relative to the stable isomer. It is difficult for the pseudorotation reaction to proceed as shown in the experiment because of the high-energy barrier and the shape of the potential energy curve. The high barrier comes mainly from the fact that one $CH_3$ group occupies the apical position.

**$P(O_2C_2H_4)H_3$ and $P(OC_3H_6)H_3$.** Westheimer[2] also discussed compounds having the ring structures shown in Figure 2, c and d. As a model of the cyclic intermediate in a RNA hydrolysis reaction, we studied the ethyleneglycoxyphosphorane ($P(O_2C_2H_4)H_3$). One end of the ring of this molecule occupies the apical position and the other end forms one end of the equatorial plane in the ground state. The angle between apical PO and PH bonds comes close as the pseudorotation reaction proceeds. The transition state has $C_s$ symmetry which resembles the $C_{4v}$ structure of a simple pentacoordinated molecule such as $PH_5$ and $PF_5$. The

**Table I.** Calculated Energies in Some Levels

$PH_5$ TZP Basis Set

| methods | calcd energies (au) ground state | calcd energies (au) transition state | rel energy (kcal/mol) | methods | calcd energies (au) ground state | calcd energies (au) transition state | rel energy (kcal/mol) |
|---|---|---|---|---|---|---|---|
| SCF | −343.528 616 | −343.524 348 | 2.68 | MP4(SDTQ) | −343.728 719 | −343.726 277 | 1.53 |
| MP2 | −343.693 636 | −343.690 815 | 1.77 | SDCI | −343.715 483 | −343.712 706 | 1.74 |
| MP3 | −343.720 720 | −343.718 088 | 1.65 | SDCI (Davidson's corr) | −343.728 684 | −343.726 360 | 1.46 |
| MP4(DQ) | −343.724 957 | −343.722 374 | 1.62 | coupled cluster | −343.725 743 | −343.723 208 | 1.59 |
| MP4(SDQ) | −343.725 823 | −343.723 284 | 1.59 | | | | |

$PF_5$ DZP Basis Set

| methods | calcd energies (au) ground state | calcd energies (au) transition state | rel energy (kcal/mol) | methods | calcd energies (au) ground state | calcd energies (au) transition state | rel energy (kcal/mol) |
|---|---|---|---|---|---|---|---|
| SCF | −838.184 055 | −838.175 975 | 5.07 | MP4(SDQ) | −839.157 117 | −839.150 024 | 4.45 |
| MP2 | −839.145 335 | −839.138 455 | 4.32 | MP4(SDTQ) | −839.183 257 | −839.176 493 | 4.24 |
| MP3 | −839.134 876 | −839.127 467 | 4.65 | SDCI | −838.999 488 | −838.991 797 | 4.83 |
| MP4(DQ) | −839.141 543 | −839.134 182 | 4.62 | SDCI (Davidson's corr) | −839.149 570 | −839.142 333 | 4.54 |

$PF_4H$ DZP Basis Set

| methods | calcd energies (au) ground state | calcd energies (au) transition state | rel energy (kcal/mol) | methods | calcd energies (au) ground state | calcd energies (au) transition state | rel energy (kcal/mol) |
|---|---|---|---|---|---|---|---|
| SCF | −739.263 577 | −739.251 810 | 7.38 | MP4(DSQ) | −740.082 283 | −740.072 611 | 6.07 |
| MP2 | −740.066 801 | −740.057 365 | 5.92 | MP4(SDTQ) | −740.103 597 | −740.094 516 | 5.70 |
| MP3 | −740.062 518 | −740.052 423 | 6.33 | SDCI | −739.962 596 | −739.952 088 | 6.59 |
| MP4(DQ) | −740.069 250 | −740.059 178 | 6.32 | SDCI (Davidson's corr) | −740.076 286 | −740.066 540 | 6.12 |

$PF_3H_2$ DZP Basis Sets

| methods | calcd energies (au) isomer A | calcd energies (au) transition state | calcd energies (au) isomer B | methods | methods | calcd energies (au) isomer A | calcd energies (au) transition state | calcd energies (au) isomer B | methods |
|---|---|---|---|---|---|---|---|---|---|
| SCF | −640.339 311 | −640.319 940 | −640.320 136 | MP4 (SDQ) | MP4 (SDQ) | −641.002 782 | −640.985 444 | −640.984 945 | |
| MP2 | −640.983 482 | −640.966 482 | −640.965 907 | | MP4 (SDTQ) | −641.019 130 | −641.002 503 | −641.001 888 | |
| MP3 | −640.986 074 | −640.968 355 | −640.967 983 | | SDCI | −640.917 403 | −640.899 434 | −640.899 221 | |
| MP4 (DQ) | −640.992 684 | −640.974 932 | −640.974 537 | | SDCI (Davidson's corr) | −640.998 586 | −640.981 249 | −640.980 803 | |

| methods | rel energies to isomer A (kcal/mol) transition state | rel energies to isomer A (kcal/mol) isomer B | methods | rel energies to isomer A (kcal/mol) transition state | rel energies to isomer A (kcal/mol) isomer B |
|---|---|---|---|---|---|
| SCF | 12.16 | 12.03 | MP4 (SDQ) | 10.88 | 11.19 |
| MP2 | 10.67 | 11.03 | MP4 (SDTQ) | 10.43 | 10.82 |
| MP3 | 11.12 | 11.35 | SDCI | 11.28 | 11.41 |
| MP4 (DQ) | 11.14 | 11.39 | SDCI (Davidson's corr) | 10.88 | 11.16 |

$PF_4CH_3$ DZP Basis Set

| methods | calcd energies (au) ground state | calcd energies (au) transition state | rel energy (kcal/mol) | methods | calcd energies (au) ground state | calcd energies (au) transition state | rel energy (kcal/mol) |
|---|---|---|---|---|---|---|---|
| SCF | −778.317 482 | −778.309 098 | 5.26 | MP4 (DQ) | −779.256 377 | −779.249 252 | 4.47 |
| MP2 | −779.243 283 | −779.236 814 | 4.06 | MP4 (SDQ) | −779.270 468 | −779.263 708 | 4.24 |
| MP3 | −779.249 062 | −779.241 875 | 4.51 | MP4 (SDTQ) | −779.295 633 | −779.289 336 | 3.95 |

$PF_3C_2H_6$ DZP Basis Set

| methods | calcd energies (au) ground state | calcd energies (au) 122.5° | rel energy (kcal/mol) | methods | calcd energies (au) ground state | calcd energies (au) 122.5° | rel energy (kcal/mol) |
|---|---|---|---|---|---|---|---|
| SCF | −718.444 972 | −718.420 999 | 15.04 | MP4 (DQ) | −719.365 328 | −719.342 659 | 14.23 |
| MP2 | −719.335 317 | −719.313 707 | 13.56 | MP4 (SDQ) | −719.377 661 | −719.355 332 | 14.01 |
| MP3 | −719.357 558 | −719.334 828 | 14.26 | | | | |

$PO_5H_4^-$ DZP + Diffusion (on Phosphonyl O) Basis Set

| methods | calcd energies (au) A | calcd energies (au) TS1 | calcd energies (au) B | calcd energies (au) TS2 | methods | calcd energies (au) A | calcd energies (au) TS1 | calcd energies (au) B | calcd energies (au) TS2 |
|---|---|---|---|---|---|---|---|---|---|
| SCF | −717.543 764 | −717.540 558 | −717.562 121 | −717.551 127 | MP4 (DQ) | −718.584 464 | −718.581 140 | −718.600 412 | −718.590 297 |
| MP2 | −718.577 403 | −718.574 347 | −718.592 420 | −718.582 677 | MP4 (SDQ) | −718.596 275 | −718.592 979 | −718.611 530 | −718.601 662 |
| MP3 | −718.576 367 | −718.573 054 | −718.592 565 | −718.582 292 | | | | | |

| methods | rel energies to isomer B state (kcal/mol) A | rel energies to isomer B state (kcal/mol) TS1 | rel energies to isomer B state (kcal/mol) TS2 | methods | rel energies to isomer B state (kcal/mol) A | rel energies to isomer B state (kcal/mol) TS1 | rel energies to isomer B state (kcal/mol) TS2 |
|---|---|---|---|---|---|---|---|
| SCF | 11.52 | 13.53 | 6.90 | MP4 (DQ) | 10.01 | 12.09 | 6.35 |
| MP2 | 9.42 | 11.34 | 6.11 | MP4 (SDQ) | 9.57 | 11.64 | 6.19 |
| MP3 | 10.16 | 12.24 | 6.45 | | | | |

$P(O_2C_2H_4)H_3$ DZP Basis Set

| methods | calcd energies (au) ground state | calcd energies (au) transition state | rel energy (kcal/mol) | methods | calcd energies (au) ground state | calcd energies (au) transition state | rel energy (kcal/mol) |
|---|---|---|---|---|---|---|---|
| SCF | −570.259 906 | −570.256 207 | 2.32 | MP4 (DQ) | −571.043 240 | −571.040 223 | 1.89 |
| MP2 | −571.006 186 | −571.003 244 | 1.85 | MP4 (SDQ) | −571.051 341 | −571.048 432 | 1.83 |
| MP3 | −571.036 013 | −571.033 022 | 1.88 | | | | |

**Table I** (Continued)

$P(OC_3H_6)H_3$ DZP Basis Set

| methods | calcd energies (au) ground state | calcd energies (au) 120.0° | rel energy (kcal/mol) | methods | calcd energies (au) ground state | calcd energies (au) 120.0° | rel energy (kcal/mol) |
|---|---|---|---|---|---|---|---|
| SCF | -534.399 504 | -534.384 867 | 9.18 | MP4 (DQ) | -535.153 406 | -535.140 562 | 8.06 |
| MP2 | -535.103 777 | -535.091 700 | 7.58 | MP4 (SDQ) | -535.159 715 | -535.147 335 | 7.77 |
| MP3 | -535.146 680 | -535.133 687 | 8.15 | | | | |

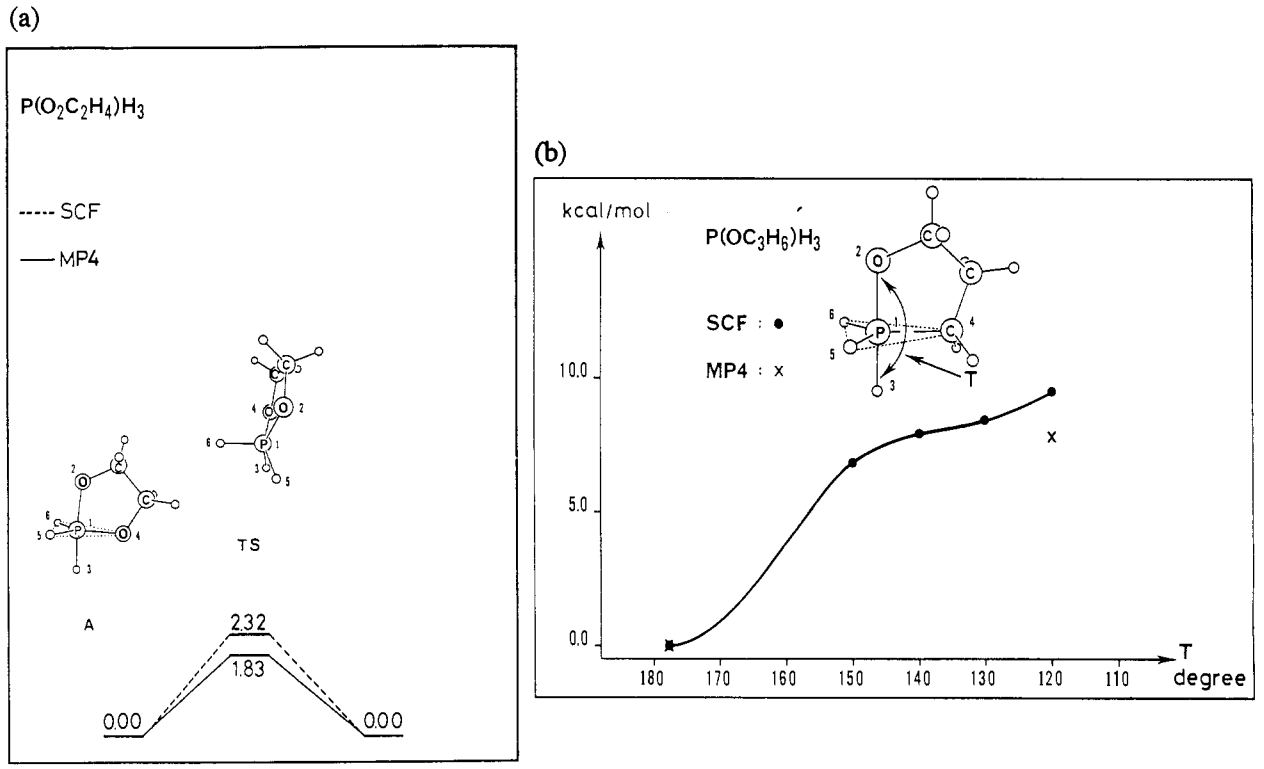


**Figure 12.** (a) Energy diagram of the pseudorotation reaction of the $P(O_2C_2H_4)H_3$ model molecule in kcal/mol. The SCF energy of the ground state A is -570.259 906 hartrees. (b) Potential energy curve of the $P(OC_3H_6)H_3$ molecule for the pseudorotation reaction in kcal/mol. The SCF energy of the ground state is -534.399 504 hartrees.

**Table II.** Potential Energy Change with SCF Calculations for $PF_3H_2$, $PF_3C_2H_6$, and $P(OC_3H_6)H_3$

| degree | total energy (au) | rel energy au | rel energy kcal/mol |
|---|---|---|---|
| | 1. $PF_3H_2$ | | |
| 178.8 (minimum 1) | -640.339 311 | 0.000 000 | 0.00 |
| 160.0 | -640.327 938 | 0.011 373 | 7.14 |
| 145.0 | -640.320 708 | 0.018 603 | 11.67 |
| 136.0 (TS) | -640.319 940 | 0.019 371 | 12.16 |
| 130.0 | -640.320 064 | 0.019 247 | 12.08 |
| 125.8 (minimum 2) | -640.320 136 | 0.019 175 | 12.03 |
| 120.0 | -640.319 871 | 0.019 440 | 12.20 |
| | 2. $PF_3C_2H_6$ | | |
| 175.3 (minimum) | -718.444 974 | 0.000 000 | 0.00 |
| 155.0 | -718.430 836 | 0.014 138 | 8.87 |
| 135.0 | -718.422 170 | 0.022 804 | 14.31 |
| 130.0 | -718.421 659 | 0.023 315 | 14.63 |
| 125.0 | -718.421 252 | 0.023 722 | 14.89 |
| 122.5 | -718.421 002 | 0.023 972 | 15.04 |
| | 3. $P(OC_3H_6)H_3$ | | |
| 177.8 (minimum) | -534.399 504 | 0.000 000 | 0.00 |
| 150.0 | -534.388 692 | 0.010 812 | 6.78 |
| 140.0 | -534.386 962 | 0.012 542 | 7.87 |
| 130.0 | -534.385 960 | 0.013 544 | 8.50 |
| 120.0 | -534.384 867 | 0.014 637 | 9.18 |

**Table III.** Change of the Bond Length (Å)

| | before reaction | transition state | after reaction |
|---|---|---|---|
| | a. $PH_5$ | | |
| pivotal length | 1.415 (100) | 1.394 (98.5) | 1.415 (100) |
| equatorial length | 1.415 (100) | 1.451 (102.5) | 1.477 (104.4) |
| | b. $PF_5$ | | |
| pivotal length | 1.537 (100) | 1.524 (99.2) | 1.537 (100) |
| equatorial length | 1.537 (100) | 1.562 (101.6) | 1.577 (102.6) |

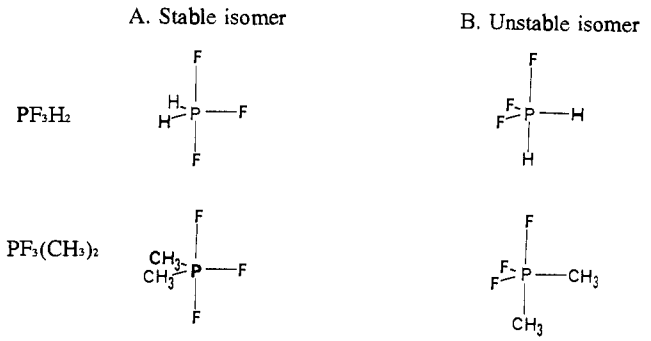


**Figure 13.** Structures of the stable (A) and unstable (B) isomers of $PF_3H_2$ and $PF_3(CH_3)_2$.

energy diagram of the pseudorotation is shown in Figure 12a. A low potential barrier is found in the pseudorotation reaction. The relative energy of the transition state to the ground state is calculated to be only 2.32 kcal/mol (SCF) and 1.83 kcal/mol (MP4), respectively. Thus it is expected that the isomerization easily occurs by the pseudorotation reaction.

We also studied another cyclic phosphorane, $P(OC_3H_6)H_3$, in which one oxygen atom of ethyleneglycoxyphosphorane is replaced by a methylene group. There is only one stable energy minimum structure in which the oxygen occupies the apical position and the carbon atom is placed in the equatorial plane. We calculated the energy change when the angle O2P1H3 is changed. The

**Table IV.**

(1) Total Energy Change of $PF_3H_2$ (hartrees)

| | separated ligand | equatorial plane formation ($PH_2F^b$ and $PF_2H^c$) | whole molecule formation |
|---|---|---|---|
| A. $E$(stable) | −639.877 916 | −640.003 001 | −640.320 136 |
| B. $E$(unstable) | −639.877 916 | −640.053 428 | −640.339 311 |
| $E$(A) − $E$(B)[a] | 0.000 000 | 0.050 427 | 0.019 175 |
| | (0.00) | (31.64) | (12.03) |

(2) Total Energy Change of $PF_3(CH_3)_2$ (hartrees)

| | separated ligand | equatorial plane ($P(CH_3)_2F^d$ and $PF_2CH_3^e$) | whole molecule formation |
|---|---|---|---|
| A. $E$(stable) | −717.992 666 | −718.110 894 | −718.420 999 |
| B. $E$(unstable) | −717.992 666 | −718.131 585 | −718.444 972 |
| $E$(A) − $E$(B)[a] | 0.000 000 | 0.020 691 | 0.023 973 |
| | (0.00) | (12.98) | (15.04) |

[a] The values in parentheses are shown in kcal/mol. [b] Equatorial plane part of the stable isomer of $PF_3H_2$. [c] Equatorial plane part of the unstable isomer of $PF_3H_2$. [d] Equatorial plane part of the stable isomer of $PF_3(CH_3)_2$. [e] Equatorial plane part of the unstable isomer of $PF_3(CH_3)_2$.

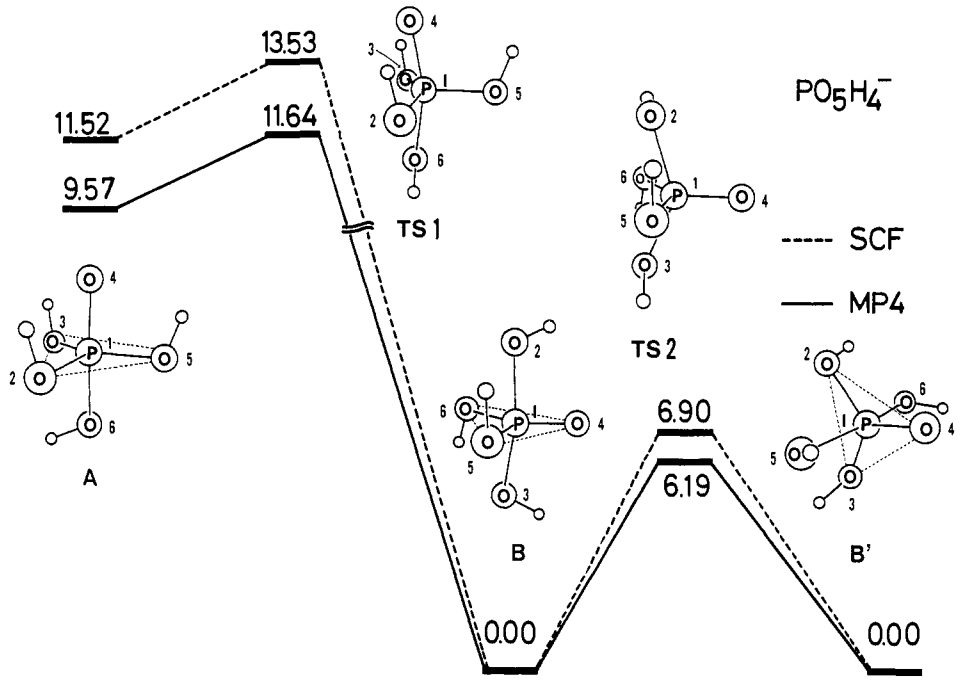


**Figure 14.** Energy diagram of the pseudorotation reaction of $PO_5H_4^-$ in kcal/mol. The phosphoryl oxygen occupies the apical position in isomer A, and it is contained in the equatorial plane in isomer B. The SCF energy of the isomer B is −717.562 121 hartrees.

results are shown in Figure 12b as a potential energy curve. There is no second stable isomer in which the carbon atom occupies the apical position and the oxygen atom occupies the equatorial one. The calculated energy barrier for the pseudorotation is about 9 kcal/mol in the SCF level. Thus the pseudorotation reaction is not expected to occur easily. When the correlation energy is taken into account, the potential barrier is reduced to 7.77 kcal/mol. The potential energy barrier becomes low, but the pseudorotated isomer will return to the ground state because of the shape of the potential surface. In the process of the pseudorotation reaction, the methylene group which forms covalent bond with the central phosphorus cannot keep the equatorial position. This bond is transferred to the apical position and stretched, and the molecule becomes unstable.

**B. Equatoriphilicity.** Here we explain the relation between the structure and the stability of the pentacoordinated phosphorus compound. Let five atoms (ligands) around P be placed a large distant apart. If we suppose that those atoms (ligands) are able to form a stable pentacoordinated molecule, we shall obtain a stabilization energy. It will be convenient to divide this into two processes, the first one corresponding to formation of the equatorial plane and the second one corresponding to formation of a pentacoordinated whole molecule. The results on $PF_3H_2$ and $PF_3(CH_3)_2$ are summarized in Table IV. In this table the separated ligand means the case in which the ligands are far apart from the central P. We name the process in which the equatorial plane parts are formed as the equatorial plane formation. The process of the whole pentacoordinated molecule formation is called a whole molecule formation. For energy calculation we used UHF method. $E$(stable) and $E$(unstable) of Table IV mean the total energy of the stable and unstable isomers, respectively. The value in $E$(A) − $E$(B) is the difference between $E$(stable) and $E$(unstable), that is, the relative stability to the stable isomer. The structures of stable and unstable molecules are shown in Figure 13. The energy of the separated ligand is the sum of the energies of all separated ligands and that of the phosphorus atom. The energy of the equatorial plane formation is the sum of the total energy of the equatorial part and those of the separated apical ligands.

In the case of $PF_3H_2$, the stable isomer is more stable by 12.03 kcal/mol than the pseudorotated unstable one. When the stabilization energies are compared in the formation of the equatorial plane ($PH_2F$ and $PF_2H$), the stabilization energy of the $PH_2F$, which is an equatorial plane of the stable isomer, is 31.64 kcal/mol greater than that of $PF_2H$. In the apical bond formation $E$(stable) of the $PF_2H$ + FH process obtains more stabilization by 19.61 kcal/mol than $E$(unstable) of the $PH_2F$ + $F_2$. The total stabilizations are obtained by adding up the two stabilization energies. The stability of the equatorial plane mainly determines the total stabilization of the pentacoordinated whole molecule. We can see a similar tendency in the case of $PF_3(CH_3)_2$, in which the total stabilization is mainly determined by the stability of the equatorial plane.

**Table V.** Relationship between the Possibility of Pseudorotation and the Number of the Equatoriphilic Groups

| no. of equatoriphilic groups | pseudorotation | some examples |
|---|---|---|
| | (a) Acyclic Molecules | |
| 0 | yes | $PF_5$ |
| 1 | yes | $PF_4CH_3$, $PF_4H$ |
| 2 | no | $PF_3(CH_3)_2$, $PF_3H_2$ |
| 3 | no | $PF_2(CH_3)_3$ |
| 4 | no | $PF(CH_3)_4$ |
| 5 | yes | $PH_5$, $P(CH_3)_5$ |
| | (b) Cyclic Molecules | |
| 0 | yes | $P(O_2C_2H_2)H_3$ |
| 1 | no | $P(OC_3H_6)H_3$ |
| 2 | yes | $P(C_4H_8)H_3$ |

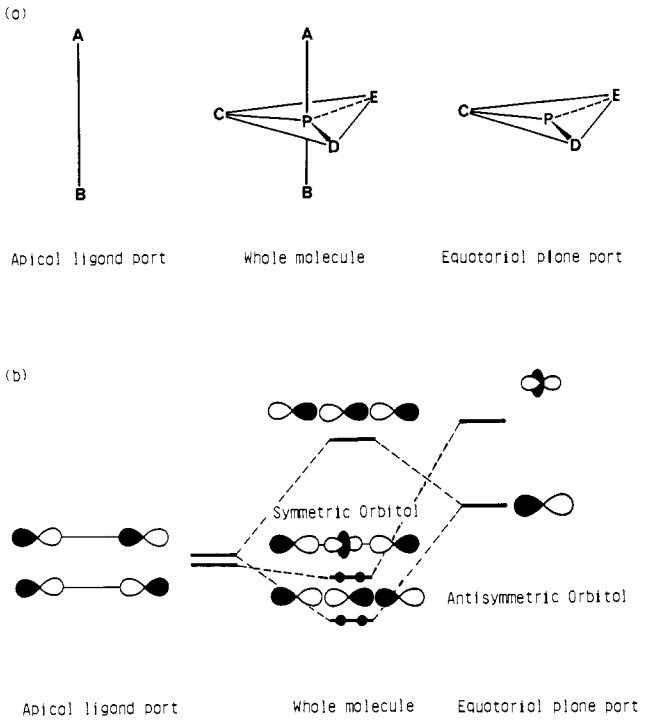


**Figure 15.** (a) Explanation of the method of division of a whole molecule into an apical part and an equatorial plane. (b) The schematic explanation of the orbital interaction of $D_{3h}$ trigonal bipyramidal molecule.

These results come from the fact that ligands such as hydrogen, methyl, and methylene, which form covalent bonds with the central phosphorus, prefer to coordinate on the equatorial positions. We name this concept as an *equatoriphilicity*. If the molecule contains only one equatoriphilic group, it occupies the pivotal position and its bond length formed with P remains almost constant through the pseudorotation reaction. But when there are more than one such ligand, one ligand at least must be moved to the apical position, and the covalent bond is lengthened in the reaction process. Thus the pseudorotated isomer becomes less stable. The number of such groups determines the possibility of the pseudorotation reaction. This explains the relationship between the ligand position and the stability of the molecule in a different viewpoint from the known apicophilicity, which says the more electronegative ligand prefers to occupy the apical position. The apicophilicity is defined based on the total energy difference of pentacoordinated molecules and widely used to discuss the stability of the isomers,[14,23] but the reason for stabilization of the whole pentacoordinated molecule is not necessarily made clear by means of the apicophilicity, while our equatoriphilicity states that the stabilization energy of the pentacoordinated molecule comes mainly from equatorial bond formation. This explains the source of the stabilization of the molecule from a more detailed point than that of the apicophilicity. We will discuss the apicophilicity in some detail in sections 3C and 3D.

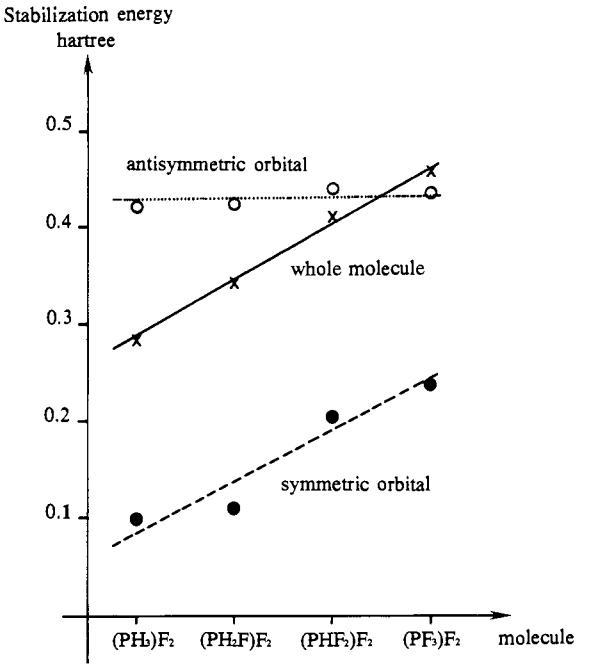


**Figure 16.** Stabilization energy of the whole molecule (full line), antisymmetric (dotted line), and symmetric (broken line) orbitals. The symbols in parentheses mean the equatorial plane part of the pentacoordinated molecule.

We present some predictions of the relation between the possibility of pseudorotation and the number of equatoriphilic groups in Table V. In acyclic molecules, when the number of the equatoriphilic groups is zero or one, the reaction is expected to occur as shown in $PF_5$, $PF_4H$, and $PF_4CH_3$. In the case of two, three, and four equatoriphilic groups, the pseudorotation reaction brings the equatoriphilic group to the apical position and so the reaction is prohibited. When all the ligands are replaced by the equatoriphilic group, the energy change before and after the pseudorotation reaction is zero, and thus the reaction will not be hindered although the resultant pentacoordinated molecule is less stable. For example, $PH_5$ is a metastable molecule, not a global one.[10] In cyclic molecules, when the number of the equatoriphilic end of the ring is zero or two, the reaction is expected to proceed. On the other hand, if the number is one, the reaction will be prohibited.

We applied the equatoriphilicity to the pseudorotation reaction of $PO_5H_4^-$. This molecule is a prototype of the pentacoordinated intermediate of the hydrolysis reaction of phosphates. There are two possible structures. One is that the phosphoryl oxygen atom is placed in the equatorial plane. The phosphoryl oxygen occupies an axial position in the other isomer. The energy relation is shown in Figure 14 with the transition state between the two isomers. The energy of the isomer A relative to the isomer B is considerably high, i.e., 11.52 kcal/mol at the SCF level and 9.57 kcal/mol even at the MP4 level. The transition-state energy between these stable isomers is calculated to be 13.53 kcal/mol (SCF) and 11.64 kcal/mol (MP4), respectively. The relative energy of the transition state to the isomer A is computed as 2.01 kcal/mol (SCF) and 2.07 kcal/mol (MP4). If isomer A is formed in the reaction of $PO_4H_3$ with the $OH^-$ anion, it isomerizes easily to the very stable product B. The phosphoryl PO bond is in the apical position in isomer A. In this structure the covalent bond is in the apical position and is lengthened. Thus the necessity of the equatoriphilicity is not satisfied in this structure, so it isomerizes to the most stable isomer B through the pseudorotation to transfer the phosphoryl PO bond to the equatorial position. We also consider the pseudorotation reaction between the isomers B and the pseudorotated B′ in which the apical axis is pseudorotated by 90°. The transition state between them is the $C_4$ symmetry structure. The transition-state energy is 6.90 kcal/mol (SCF) and 6.19 kcal/mol (MP4) higher than that of the isomer B. This result implies that the intermediate of the hydrolysis reaction of the

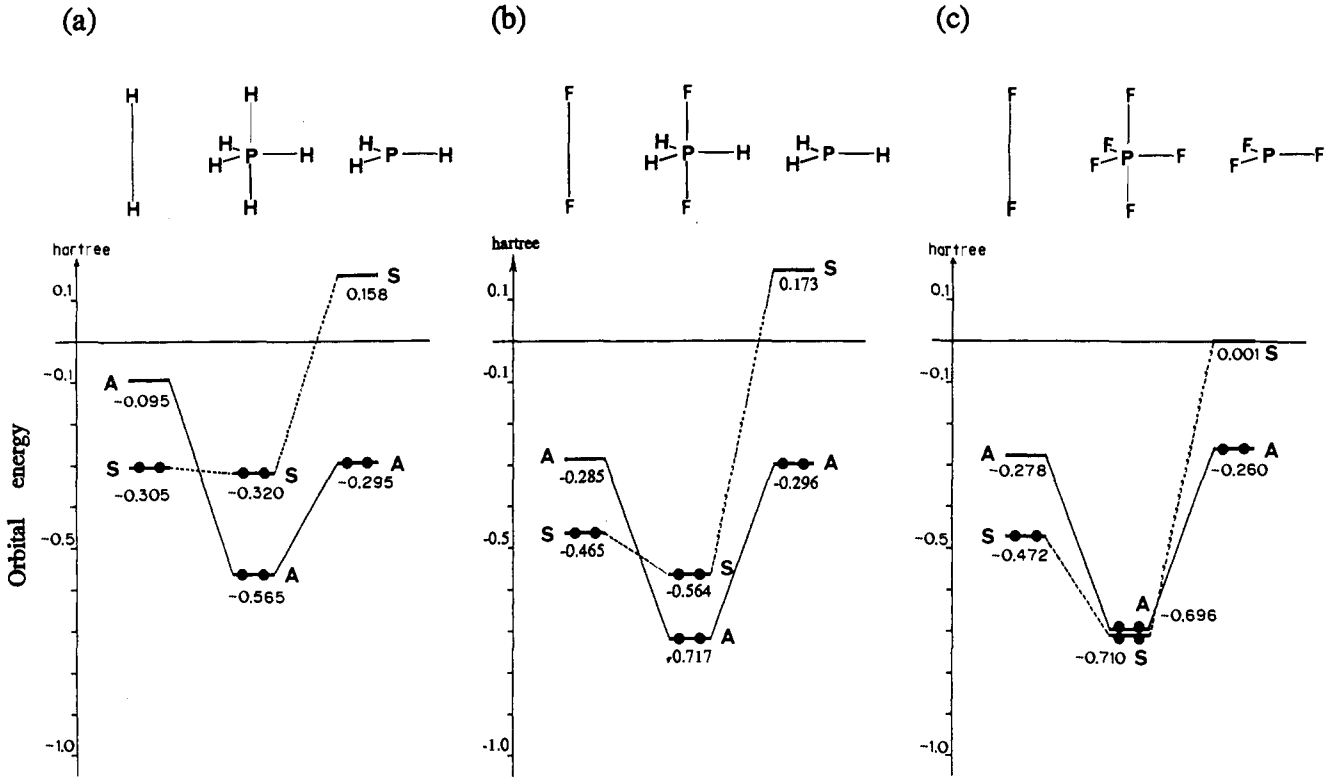


**Figure 17.** Orbital energy correlation diagrams of (a) $PH_5$, (b) $PH_3F_2$, and (c) $PF_5$. The S and A mean the symmetric and antisymmetric orbitals about the equatorial plane.

phosphate will easily isomerize by pseudorotation.

**C. Apical Bonding Character.** We divided a whole molecule into an equatorial plane and an apical ligand part as shown in Figure 15a and drew molecular orbital energy correlation diagrams between them in order to study the character of the apical bond and the origin of the well-known apicophilicity (see Figure 15b). Here an orbital which is symmetric about the equatorial plane is called a symmetric orbital. An antisymmetric orbital means an antisymmetric one about the equatorial plane. When a whole molecule A–B is formed from two parts, A and B, their orbitals $\varphi_a$ and $\varphi_b$, having the orbital energies $\epsilon_a$ and $\epsilon_b$ ($\epsilon_a < \epsilon_b$), respectively, interact to yield two new orbitals $\varphi_a'$ and $\varphi_b'$. Through the orbital interaction, the energy level of the orbital $\varphi_a'$ is lowered relative to that of the initial orbital $\varphi_a$ by the value $\Delta\epsilon_a$ estimated with second-order perturbation theory

$$\Delta\epsilon_a = \epsilon_a' - \epsilon_a = \frac{(H_{ab} - \epsilon_a S_{ab})^2}{\epsilon_a - \epsilon_b} \qquad (1)$$

where $H_{ab}$ is the interaction energy and $S_{ab}$ is the overlap integral for these orbitals.[51] The factors affecting the orbital stabilization are the orbital overlapping and the energy level closeness of the interacting two orbitals $\varphi_a$ and $\varphi_b$.

The graph in Figure 16 shows the stabilization of the total energy, symmetric and antisymmetric orbital energies in the formation of the pentacoordinated molecule. The stabilization energies are plotted versus the change of the number of the equatorial fluorine atoms. Both of two apical ligands are fixed to fluorine atoms. The symbols in the parentheses mean the equatorial plane parts. The relation between the total energy and the orbital energies is given by

$$E_{tot} = 2\sum_{i}^{occ}\epsilon_i - V_{ee} + V_{nn} \qquad (2)$$

where $E_{tot}$, $\epsilon_i$, $V_{ee}$, and $V_{nn}$ mean total energy, $i$th orbital energy, electronic and nuclear repulsive interaction, respectively. We can easily see that the close relation between the equatorial substituent effect on the symmetric orbital and that on the whole molecule. On the other hand, the stabilization energies of the antisymmetric orbitals are almost same for every case. There is little substituent effect on the antisymmetric orbital from the equatorial fluorine.

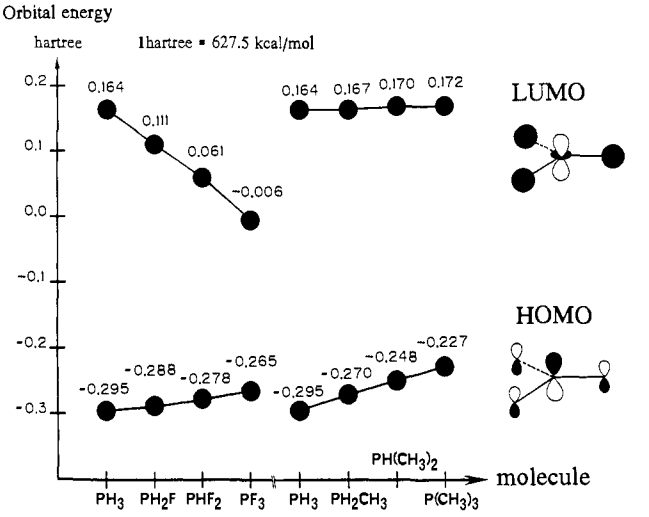


**Figure 18.** Substituent effect on HOMO and LUMO of the equatorial part. The orbital energy is shown in atomic unit.

Thus we can discuss the molecular stabilization by using only the symmetrical orbital stabilization.

This result can be explained as follows. The electrons in the antisymmetric orbital concentrate on the $3p_z$ lone pair of the central phosphorus before the orbital interaction. The orbital interaction stabilizes the system by extension of the orbital space. Therefore, if the same apical ligands are coordinated, the almost same stabilization will be given by the orbital interaction. This antisymmetric orbital interaction explains the origin of the well-known apicophilicity[14] so far mainly related with the electronegativity of the apical ligand. If the electronegative and electron-withdrawing group is placed in the apical position, the electrons concentrated on the $3p_z$ lone pair of the phosphorus move to the apical bond region, and a strong ionic bond is formed with great stabilization. On the other hand, the symmetric electrons are on the stretched apical ligands before the orbital interaction. The $3d_{z^2}$ AO of the central phosphorus bridges two apical fluorines through the symmetric orbital interaction, and thus its contribution

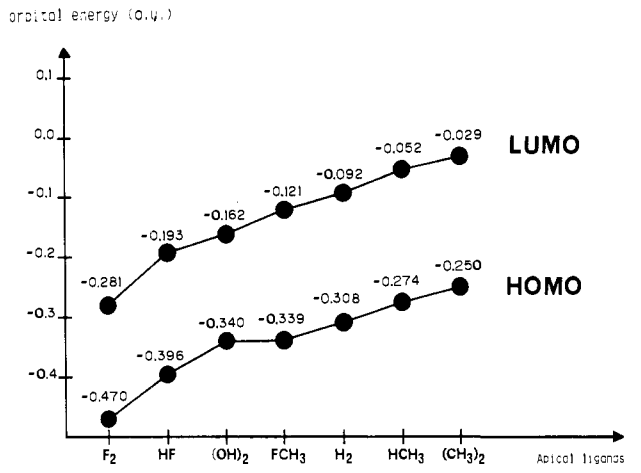


**Figure 19.** Orbital energy variations of some apical ligands part. The orbital energy is shown in atomic units.

is essentially important for the stabilization of the axial bond. Thus there are obvious differences in the stabilization of the symmetric orbital owing to the differences in the ability of participating in the three-center bond.

The orbital energy correlation diagrams of $PH_5$, $PH_3F_2$, and $PF_5$ are shown in Figure 17, a, b, and c, respectively. In $PH_5$ the symmetric orbital is characterized by the 1s AO of the apical hydrogen and $3d_{z^2}$ orbital of the central phosphorus atom mixed into it. This orbital is slightly stabilized because the $3d_{z^2}$ AO of the central phosphorus is in a high-energy level. There is the difficulty of inducing the charge transfer from the donor $H_2$ to the acceptor $PH_3$.

In $PH_3F_2$ the stabilization of the A orbital is much larger than that of $PH_5$. This means that the fluorine is the more apicophilic ligand. The stabilization of the S orbital mainly comes from the interaction of the 2p AO of the apical fluorine and $3d_{z^2}$ AO of the central phosphorus atom. The charge transfer from the HOMO of fluorine to the LUMO of the phosphorus atom is induced strongly by this contribution of the $3d_{z^2}$ AO. The larger stabilization of the antisymmetric orbital induces the great charge transfer from the lone-pair HOMO of $PH_3$ to the LUMO of $F_2$, as the difference of the electronegativity is large (2.19 for P and 3.98 for F by Pauling's definition).[52] Because of the charge transfer, almost all the electrons on the phosphorus HOMO flow to the apical LUMO, and the coefficients of the $3p_z$ AO of the central phosphorus in the whole $PH_3F_2$ molecule become small and the bond with ionic character is formed in P–F regions.

In $PF_5$ there is a very strong substituent effect on the LUMO of the equatorial plane because all equatorial positions are substituted by fluorines. So the stabilization of symmetric orbital becomes much larger than that of $PH_5$. The stabilization of the antisymmetric orbital is almost the same with $PH_3F_2$ as the apical ligand for both molecules is fluorine; i.e., the apicophilicity is fixed.

**D. Substituent Effects.** The orbital energy level of the equatorial plane parts of the pentacoordinated molecule have an important contribution to the stabilization of the apical bond. We studied the substituent effect on the apical orbital of the equatorial plane part.

The results of the substituent effects on the HOMO and LUMO of the equatorial part are shown in Figure 18. The bond angles in the triangle plane are fixed to be 120°. All combinations of equatorial ligands are considered by using the following bond lengths: $R$(P–H) = 1.40 Å, $R$(P–F) = 1.55 Å, and $R$(P–$CH_3$) = 1.81 Å. When a fluorine atom coordinates as an equatorial ligand, the oribtal energy of LUMO becomes lower. On the other hand, there is not an obvious effect of an equatorial ligand in the case of the methyl group and hydrogen atom. The substituent effect on the LUMO comes from the $\sigma$-type attracting interaction with ligands. When strong electronegative ligands like fluorine coordinate, the $\sigma$-type interaction is induced and the orbital energy of the LUMO becomes lower. Thus if the apical ligands are fixed, there is much stabilization of the axial orbital in molecules having fluorine as an equatorial ligand. The axial bond becomes strong in such molecules. The influence of the substituent to HOMO of the equatorial part comes from the $\pi$-type donating interaction to the $3p_z$ lone pair of the central phosphorus atom. When the methyl group coordinates, its effect is given through hyperconjugation. The orbital energy of the HOMO becomes higher as the antibonding nature through the $\pi$-type interaction increases, though this effect is smaller than that of the $\sigma$-type interaction in the LUMO.

We showed the variation of the orbital energies of the apical LUMO according to the difference of the apical ligand in Figure 19. In this study, one dummy atom is defined at a middle point of the apical bond. The bond lengths from a dummy atom (X) to each apical ligands are as follows: $R$(X–H) = 1.45 Å, $R$(X–F) = 1.60 Å, $R$(X–$CH_3$) = 1.84 Å, and $R$(X–OH) = 1.74 Å. The interaction between the $3p_z$ HOMO of the central phosphorus and LUMO of the apical ligand becomes greater when the electronegative ligands participate in the interactions because of their low orbital energies of LUMO. If the equatorial part is kept fixed, the molecule having fluorines as apical ligand is most stable and that having hydrogen atoms or methyl groups is less stable. The variation of the orbital energy of the apical ligand gives a significant influence to the strength of the apicophilicity.

## 4. Conclusions

The implications of this study can be summarized as follows.

1. By analyzing the energy relation between the stable isomer and the unstable one in the pseudorotation reaction, we found that the stabilization of the equatorial plane part of the pentacoordinated molecule determines the stability of the whole molecule. The groups forming the covalent bonds with P such as H, $CH_3$, and $CH_2$ prefer to coordinate in the equatorial position, i.e., *equatoriphilicity*. If the whole molecule was formed from completely separate atoms, the equatorial plane part would be formed first by the groups which make covalent bonds with P, and then the remaining ligands would coordinate at the apical positions.

2. We drew orbital energy correlation diagrams for some molecules and considered the stability of apical bonds. The apical bond has three-center, four-electron character. When the apical ligands are fixed, the special orbital is related to the stabilization of the molecule. We can discuss the strength or nature of the apical bond by using the special orbital.

3. The potential energy barrier of the pseudorotation for the model phosphate molecule is fairly low, and it is considered that the reaction proceeds easily in the gas phase.

4. From the study of the substituent effect on the equatorial plane part, it is shown that the fluorine has a significant effect on the 3d AO of the central phosphorus.

5. The correlation effect is significant but not essential in determining the potential barrier height. The MP2 level of the energy correction seems to be adequate for some explanations of the nature of pseudorotation reactions.

**Acknowledgment.** The SCF and MP4 calculations were carried out using the Gaussian-80,[42] Gaussian-82,[43] and Gaussian-86[34] programs. The calculations were carried out on FACOM M782 and VP200 computers at Nagoya University Computational Center and on a HITAC S810 computer at the Institute for Molecular Science. This study was supported in part by a Grant-in-Aid for Scientific Research from the Japanese Ministry of Education, Science, and Culture.

**Registry No.** $PH_5$, 131232-65-0; $PF_5$, 137038-30-3; $PF_4H$, 51262-44-3; $PF_3H_2$, 38474-13-4; $PF_4CH_3$, 137038-31-4; $PF_3(CH_3)_2$, 137038-32-5; $P(O_2C_2H_4)H_3$, 127489-42-3; $P(OC_3H_6)H_3$, 135198-59-3; $PO_5H_4^-$, 125106-44-7.